

## **Stacked Microstrip Antenna Employing Tapered Multi-Ring Elements**

Tomohiro Seki, Naoki Honma, Kenjiro Nishikawa, and Kouichi Tsunekawa  
NTT Network Innovation Laboratories, NTT Corporation  
1-1 Hikari-no-oka, Yokosuka-shi, Kanagawa 239-0847, Japan  
TEL: +81 46 859 5070, FAX: +81 46 855 1497 E-mail: t.seki@ieee.org

### **1. INTRODUCTION**

System studies and hardware investigations on high-speed wireless communications are being conducted at millimeter and quasi-millimeter-wave frequencies [1]-[3]. These applications require compact, high performance, and low-cost wireless equipment. A highly integrated RF module, the so-called system-on-package module, which employs a multi-layer structure, is effective in achieving the above requirements [4]-[7]. It is necessary to adopt active integrated antenna technology to achieve a module with antennas that are low-power consuming and have low-noise characteristics [8]-[10]. Several approaches to achieve the RF module integrated with antennas were reported. One approach uses a semiconductor chip antenna such as a microstrip antenna (MSA) that is integrated with RF circuits on the same semiconductor substrate [4]. However, it is difficult to establish a high-gain antenna that employs an array antenna configuration on a semiconductor substrate due to the substrate size.

Therefore, high-gain compact antennas have not yet been integrated with monolithic microwave integrated circuits (MMICs). A multi-chip module approach was also proposed to construct a module integrated with antennas [5],[6]. In this module, antennas and MMICs are connected by wire bonding or a ribbon, which results in high connection loss. This approach also needs a low-loss feeding circuit. The dielectric lens antenna is adopted to achieve a high-gain antenna [7]. However, the commonly used lens antenna is constructed using a crystal material that is high cost and it is difficult to mount it on the MMIC package. Therefore, a dielectric lens antenna constructed using resin was investigated to decrease the cost. There are problems, however, regarding mounting the antenna on the MMIC package and achieving high efficiency.

To overcome these problems, we proposed a multi-layer parasitic MSA array structure [10],[11]. However, it is difficult to design the arrangement of the stacked parasitic patches for this antenna. Therefore, we propose a new antenna structure using a multi-layer substrate for millimeter-wave applications. The proposed antenna is based on the short backfire antenna [12], which potentially offers a high antenna gain.

In this paper, we describe a microstrip antenna structure with parasitic elements employing stacked rings, which achieves a high gain and radiation efficiency that is greater than 18.6 dBi and 97.7% at 63 GHz, respectively.

### **2. CONFIGURATION OF PROPOSED ANTENNA**

The proposed antenna structure is shown in Fig. 1. This antenna is constructed using a feeding microstrip antenna with a parasitic element and ring metals forming the reflector antennas on a multi-layer substrate. In the figure, the parasitic element is arranged on the MSA for feeding. The MSA contains a reflector, which comprises stacked rings in the multi-layer substrate to bind the reflection wave to the feeding and the parasitic element. While suppressing the total substrate thickness according to this composition, constructing a large-scale antenna is possible. In the design of this antenna, the size and the height of the

parasitic element greatly influence the antenna characteristics. Next, the design and the operation mechanism of the proposed antenna are described.

### 3. DESIGN AND PERFORMANCE OF PROPOSED ANTENNA

The design for the 60-GHz band is presented. We use the moment method as the calculation method and assume that the ground plane is infinite. For calculation, we adopt the constants of the multi-layer high temperature co-fired ceramic substrate ( $\epsilon_r = 9.0$ ,  $\tan\delta = 0.001$  at 10 GHz) that achieve a low manufacturing cost. The simulation model is shown in Fig. 2. The size of the feeding element is 0.83 mm x 0.83 mm and the feeding point is 0.135-mm away from the center of the patch. Here, we use a nine-layer stacked ring for the reflector. The radius of the metal ring at the bottom is assumed to be 2.50 mm. Additionally, the width of the metal rings of each layer is 0.75 mm and the angle of the taper is adjusted to 78.7 degrees.

First, when the size of the parasitic element is varied, the effect of the antenna characteristics is shown in Fig. 3. In this figure, it is clear that the gain and the efficiency of this antenna have the peak characteristics for the radius of the parasitic element. The calculated results of the maximum absolute gain when the reflectors are constructed with nine-layers are 18.6 dBi, and the radiation efficiency is 97.7%. Moreover, it is thought that the radiation efficiency of the antenna is improved by operating as a conventional parasitic element when the radius of the parasitic element is approximately 0.7 mm. The size of the parasitic element where the peak occurs corresponds to almost one wavelength in the dielectric substance. It is thought that the higher-order mode is excited due to this on the parasitic element.

Next, when the height of the parasitic element is varied, the effect of the antenna characteristics is shown in Fig. 4. In this figure, it is understood that two peaks exist for the height of the parasitic element. In analyzing the results of the radiation characteristics for this antenna, when the height is 0.5 mm or more, a problem occurs in which a null is generated in the main lobe.

To understand the operation of this antenna, the analytical results of the current distribution on the parasitic element of this antenna are shown in Fig. 5. In this figure, it is clear that the higher-order mode is excited on the parasitic element. Therefore, it is thought that the current can be effectively distributed on the reflector, which is constructed with the multi-ring element, without using the first reflector compared to the short backfire antenna using the microstrip antenna for the feeding element. The difference is caused by the excited mode in the current distributed through the multiple rings on the parasitic element. This causes the difference in the direction characteristics in the E-plane and H-plane.

Next, the calculated results of the E-plane and H-plane radiation patterns at 63 GHz are shown in Fig. 6. In this figure, it is clear that the half power beam width of the H-plane is 20 degrees, and that for the E-plane is 12 degrees. Moreover, it is understood that there is a large sidelobe level in the E-plane radiation pattern characteristics. It seems that it causes the difference in the current distribution on the multi-ring reflector.

### 4. CONCLUSION

We proposed a stacked microstrip antenna employing tapered multi-ring elements on a multi-layer substrate suited for the millimeter-wave system-on-package. The design and performance of the proposed antenna was described. The proposed antenna achieves the antenna gain of 18.6 dBi and its radiation efficiency is greater than 97.7%.

#### Acknowledgment

The authors thank Dr. Masahiro Umehira and Dr. Ichihiko Toyoda of NTT Network Innovation Laboratories for their helpful discussions and suggestions.

## References

- [1] Y. Takimoto, "Recent activities on millimeter wave indoor LAN system development in Japan," in IEEE MTT-S Int. Symp. Dig., pp. 405-408, June 1995.
- [2] N. Morinaga and A. Hashimoto, "Technical trend of multimedia mobile and broadband wireless access systems," Trans. IEICE., Vol. E82-B, No. 12, pp. 1897-1905, Dec. 1999.
- [3] T. Ihara and K. Fujimura, "Research and development of millimeter-wave short-range application systems," Trans., IEICE, Vol. E79-B, No. 12, pp. 1741-1753, Dec. 1996.
- [4] T. Nakagawa, K. Nishikawa, B. Piernas, T. Seki, and K. Araki, "60-GHz antenna and 5-GHz demodulator MMICs for more than 1-Gbps FSK transceivers," in 32nd European Microwave Conference Dig., pp. 929-932, Sep. 2002.
- [5] Y. Hirachi, H. Nakano, and A. Kato, "A cost-effective RF-module with built-in patch antenna for millimeter-wave wireless systems," in 29th European Microwave Conference Dig., pp. 347-350, Oct. 1999.
- [6] M. Tentzeris, N. Bushyager, J. Laskar, G. Zheng, and J. Papapolymerou, "Analysis and design of MEMS and embedded components in Silicon/LTCC packages using FDTD/MRTD for system-on-package applications system-on-package (SOP)," Digest of Silicon Monolithic Integrated Circuits in RF Systems, 2003 Topical Meeting, pp. 138-141, April 2003.
- [7] U. Sangawa, T. Urabe, Y. Kudoh, A. Omote, and K. Takahashi, "A study on a 60 GHz low profile dielectric lens antenna using high-permittivity ceramics -toward a low profile antenna," Technical report of IEICE, MW2002-116, pp. 57-62, Nov. 2002.
- [8] J. Lin, and T. Itoh, "Active integrated antennas," IEEE Trans. MTT, Vol. 42, pp. 2186-2194, Dec. 1994.
- [9] T. Seki, H. Yamamoto, T. Hori, and M. Nakatsugawa, "Active antenna using multi-layer ceramic-polyimide substrates for wireless communication systems," Digest on IEEE MTT-S 2001 Int. Microwave Symp., pp. 385-388, May 2001.
- [10] T. Seki, K. Nishikawa, and K. Cho, "Multi-layer parasitic microstrip array antenna on LTCC substrate for millimeter-wave system on-package," 33rd European Microwave Conference, 33rd European Microwave Conference, pp. 1393-1396, Oct. 2003.
- [11] T. Seki, Naoki Honma, K. Nishikawa, and K. Tsunekawa, "High Efficiency Multi-Layer Parasitic Microstrip Array Antenna on TEFLON Substrate," 34th European Microwave Conference, pp. 829-832, Oct. 2004.
- [12] M. Rayner, A.D. Olver, and A.D. Monk, "FD-TD design of short backfire antennas," IEE Proc.-Microw. Antennas Propag., Vol. 144, No. 1, pp. 1-6, Feb. 1997.

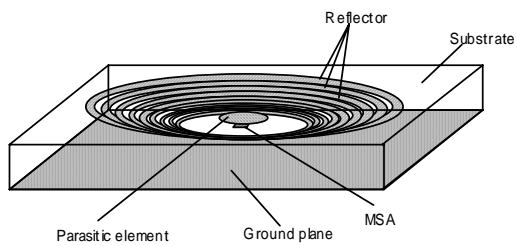


Fig. 1 Antenna model

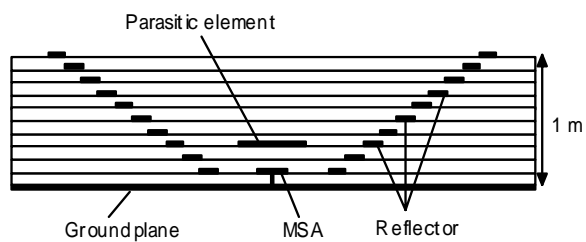


Fig. 2 Calculation model

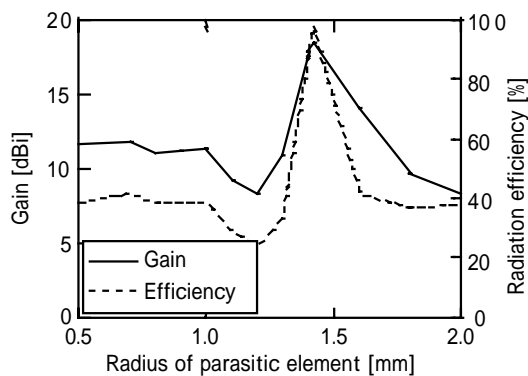


Fig. 3 Absolute gain and radiation efficiency characteristics versus parasitic element size

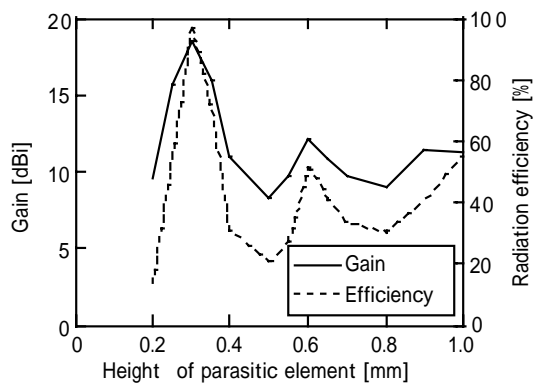


Fig. 4 Absolute gain characteristics versus height of parasitic element

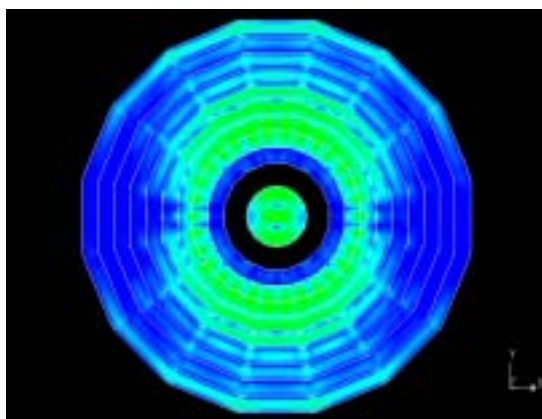


Fig. 5 Calculated results of current distribution

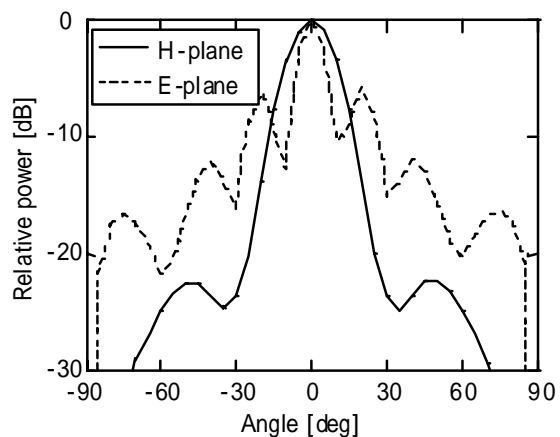


Fig. 6 Calculated radiation pattern